ELSEVIER

Ceramics International 31 (2005) 1041–1044

CERAMICS INTERNATIONAL

www.elsevier.com/locate/ceramint

Synthesis of hydroxyapatite nanoparticles in ultrasonic precipitation

Li-yun Cao*[,1], Chuan-bo Zhang[2], Jian-feng Huang

School of Material Science and Engineering, ShaanXi University of Science and Technology, Xian'yang, ShaanXi Province 712081, PR China

Received 1 September 2004; received in revised form 10 October 2004; accepted 6 November 2004
Available online 25 January 2005

Abstract

Nanocrystalline hydroxyapatite (HAp) was prepared by a precipitation method with aid of ultrasonic irradiation using $Ca(NO_3)_2$ and $NH_4H_2PO_4$ as source material and carbamide (NH_2CONH_2) as precipitator. The crystallization and morphology of the prepared nanoparticles were characterized by X-ray diffraction (XRD) and scanning electron microscopy (SEM). The mechanism and kinetics of the nano-hydroxyapatite were considered in particular, and the influence of the temperature and time on the HAp formation rate was also investigated. The results show that the needle-like HAp crystalline was prepared by the ultrasonic precipitation process. The HAp content increases with the preparation temperature and time. The adding of carbamide is helpful for formation of HAp nanoparticles. An Arrhenius relationship was found between the HAp formation rate and the temperature, and an apparent activation energy of 59.9 kJ/mol was obtained by calculation.

Keywords: A. Powders: chemical preparation; D. Apatite; Kinetics

1. Introduction

Hydroxyapatite (HAp), or $Ca_{10}(PO_4)_6(OH)_2$), has been widely considered as one of the most important bioceramics for medical and dental applications such as dental implants, alveolar bridge augmentation, orthopaedics, maxillofacial surgery and drug delivery systems due to its biocompatibility, and chemical and biological affinity with bone tissue [1–3]. To produce high quality HAp bioceramics for artificial bone substitution, ultrafine HAp powder was usually employed [4]. Nano-HAp powder results in easy handing, casting and sintering, leading to an excellent sintered body in the bioceramics preparing process.

Up to now, many methods such as sol–gel [5], homogeneous precipitation [6], hydrothermal [7], mechno-chemical [8], RF plasma spray [9], spray dry [10], combustion synthesis [11], supersonic rectangular jet impingement [12], ultrasonic spray freeze-drying [13] methods have been developed to prepare HAp powders. In these methods, wet chemical process was usually used to prepare HAp powders because it is easy to operate and need not any expensive equipments. However, it needs highly qualified and controlled parameters such as nature and composition of the starting materials, pH and temperature of the solutions prepared to obtain HAp monophase.

In the present work, nanocrystalline HAp was prepared by a novel precipitation method with aid of ultrasonic irradiation using $Ca(NO_3)_2$ and $NH_4H_2PO_4$ as source material. The crystallization and the morphology of the prepared nanopowder were primarily investigated, and the mechanism and kinetics of the nano-hydroxyapatite were particularly considered.

2. Experimental

Analytical grade $Ca(NO_3)_2$, NH_2CONH_2 and $NH_4H_2PO_4$ were selected for use in this work. A tool for irradiating ultrasound was an available commercial device (SC-III, ultrasonic irradiator, Jiu Zhou, China) with a variable power of 100–300 W. The sonic horn made of Ti (dip diame-

* Corresponding author. Tel.: +86 910 3570704; fax: +86 910 3579723.
E-mail address: cly408@163.com (L.-y. Cao).
[1] Present address: College of Chemistry and Chemical Engineering, Shaanxi University of Science and Technology.
[2] Present address: College of Resource and Environment, Shaanxi University of Science and Technology.

0272-8842/$30.00
doi:10.1016/j.ceramint.2004.11.002

ter × length = ∅ 10 mm × 70 mm) was driven by a PZT transducer.

Firstly, the $Ca(NO_3)_2$ and $NH_4H_2PO_4$ were weighed in molar ratio of Ca/P at 1.67 and dissolved in distilled water to make a homogenous solution. The starting concentration of Ca^{2+} ($[Ca^{2+}]$) was also designed at 0.02 mol/L. Then, the solution was heated with a water bath that provides an invariable reactive temperature at 333–363 K. In the meantime, the sonic horn was dipped into the solution around 10 mm apart from the bottom of the flask. In the preparation process, the sonicating power and amplitude were adjusted to provide the power output of 200 W. The periods of irradiation time (reactive time) was adjusted at 1–4 h. Next, the 12 wt.% NH_2CONH_2 solution was added to the solution to fix the solution pH in the vicinity of 7.4. After reaction for different due time, the precipitates were separated from the mother liquor by filtration, and washed with de-ionized water by four times. The filtrates were dried in a vacuum dryer for 12 h at 353 K.

The phase composition of the as-prepared powders were quantitatively identified by X-ray diffraction (XRD) using a high-resolution Seifert-FPM diffractometer operating with Cu Kα radiation at 40 kV and 40 mA, divergence slit of 1°, receiving slit width of 0.1 mm and a scan rate of 2°/min. The Debye–Scherer equation, $r = K\lambda/B \cos\theta$, was used in order to determine the crystallite sizes along (2 1 1) directions: r is the crystallite in the chosen direction, K the constant, λ the wavelength of the Cu Kα radiation and B is the line width of the XRD peak. The crystallite morphology of the samples was analyzed in a transmission electron microscope (TEM) operated at 200 kV. TEM specimens were prepared by depositing a few drops of HAp dispersed in acetone on a carbon-coated copper grid.

3. Results and discussion

3.1. XRD analysis and TEM observation

Fig. 1 displays the XRD pattern of the HAp powders prepared at 363 K, $[Ca^{2+}]$ = 0.02 mol/L, Ca/P = 1.67, 200 W ultrasonic power and 3 h reaction time. It revealed that the ultrasonic precipitation technique was a suitable method to produce HAp particles, and almost monophase of HAp was obtained after reaction for 3 h at 363 K. The nature also showed a weak peak intensity and strong orientation in (2 1 1) direction, which inferred that the as-prepared HAp might be nano-crystallites in needle-like structure. This deduction was verified by the TEM observation (Fig. 2). Fig. 2 shows the TEM image of the HAp powders prepared in different ultrasonic power. It reveals the formation of acicular particles. This is similar to the particle morphologies (acicular or plate-like) reported by other wet chemical methods [5–8]. From the TEM images, the sizes of the acicular and spherical particles were determined to be 20 nm (200–500). By XRD calculation according to the Sherrer formula, the acicular crystallite size in the perpendicular direction of the (2 1 1) Miller plane was calculated to be around 18 nm. This was comparable to the TEM micrograph.

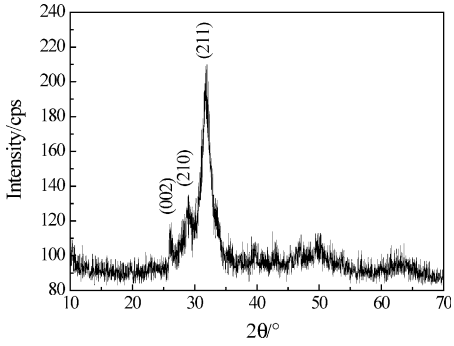

Fig. 1. The XRD pattern of the HAp powders prepared at 363 K, $[Ca^{2+}]$ = 0.02 mol/L, Ca/P = 1.67, 200 W ultrasonic power and 3 h reaction time.

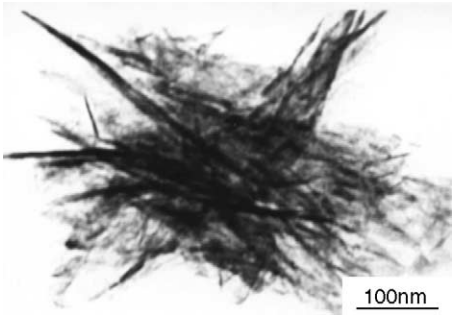

Fig. 2. The TEM image of the HAp powders prepared at 333 K, $[Ca^{2+}]$ = 0.02 mol/L, Ca/P = 1.67, 200 W ultrasonic power and 3 h reaction time.

3.2. Analysis of the reaction mechanism

Based on the HAp formation process and the opinion of many researchers [14–16], the reaction progress may be a combination of several chemical reactions.

Firstly, when the carbamide is added into the solution. There exist reactions or equilibrium reactions as follows:

$$CO(NH_2)_2 + H_2O = 2NH_3 + CO \quad (1)$$

$$NH_3 + H_2O = NH4^+ + OH^- \quad (2)$$

During the ultrasonic precipitation process, the CO_2 will be quickly escaped due to the ultrasonic irradiation, and the pH value of the solution is increased to maintain the following reaction:

$$10Ca^{2+} + 6H_2PO_4^- + 14OH^- \overset{\text{ultrasound}}{\longrightarrow} Ca_{10}(PO_4)_6 \times (OH)_2 + 12H_2O \quad (3)$$

The formation of OH^- in the solution is crucial to maintain the reaction (3).

Therefore, the continues adding of carbamide is important to obtain HAp particles, and the pH of the

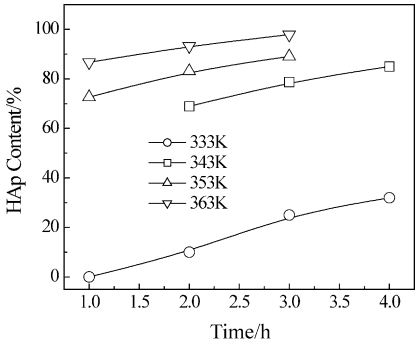

Fig. 3. The effect of reaction temperature and time on the HAp content.

solution is adjusted in the vicinity of 7.4 in order to acquire nano-HAp during the whole preparation process.

3.3. Kinetic analysis of HAp formation

According to the Arrhenius equation, the reaction rate takes the following form:

$$V = \frac{dc}{dt} = KC^n \tag{4}$$

$$K = Ae^{(-E/RT)} \tag{5}$$

where c is the HAp content, t the reaction time, K the rate constant, n the reaction order, E the activation energy, T the reaction temperature, R and A is the constant.

During the reaction time t, x% of the reagent is conversed into HAp, i.e.

$$\frac{dx}{dt} = K'(1-x)^n \tag{6}$$

$$K' = A'e^{(-E/RT)} \tag{7}$$

The HAp content, x, can be quantitatively measured using XRD after the ultrasonic precipitation reaction has been performed for a different duration (Fig. 3).

From Eqs. (6), (8) can be obtained:

$$\ln\left(\frac{dx}{dt}\right) = n\ln(1-x) + B \tag{8}$$

Using the data in Fig. 3, the linear curve $\ln(dx/dt)$ versus $\ln(1-x)$ can be plotted (Fig. 4), and the reaction order, n,

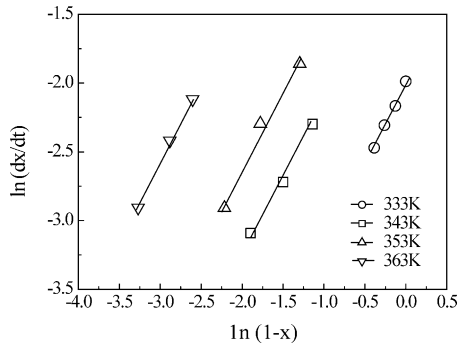

Fig. 4. The relationship between $\ln(dx/dt)$ and $\ln(1-x)$ in different reaction temperature.

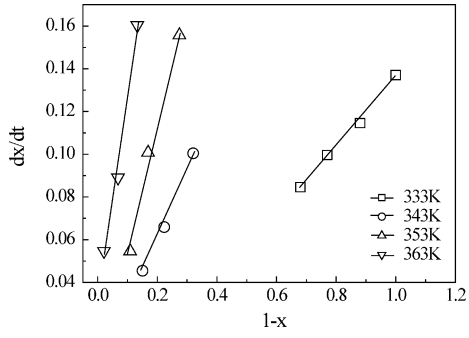

Fig. 5. The relationship between dx/dt and $(1-x)$ at different reaction temperature.

can be deduced from the slope. The results are 1.060, 1.012, 1.108 and 0.994, respectively, for reaction temperatures of 333, 343, 353 and 363 K. It follows from the calculation that the reaction may be regarded as a first order reaction (n = 1).

Substituting 1 for n in Eq. (6), the following result could be obtained:

$$\frac{dx}{dt} = K'(1-x) \tag{9}$$

By plotting (dx/dt) against $(1-x)$ (Fig. 5), K' can be calculated from the slope. The results are 0.161, 0.325, 0.603 and 0.953, respectively, at 333, 343, 353 and 363 K (Fig. 6).

Derived from Eq. (7), (10) is obtained:

$$\ln K' = -\frac{E}{RT} + \ln A' \tag{10}$$

Since the values of (E/R) and A' can be obtained from the $\ln K'$ versus $(1/T)$ curve, the apparent activation energy value, E, and the constant, A', can then be calculated. The figures obtained were 59.9 kJ/mol and 4.22×10^8, respectively.

Ultimately, the Arrhenius relationship for the conversion of $NH_4H_2PO_4$ and $Ca(NO_3)_2$ with the adding of ammonia into HAp in an ultrasonic irradiation environment becomes:

$$V = Ae^{(-E/RT)}C \tag{11}$$

where E and A are 59.9 kJ/mol and 4.22×10^8, respectively.

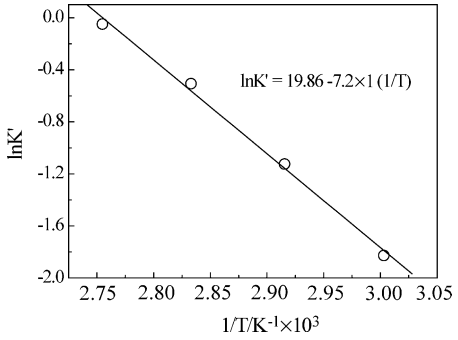

Fig. 6. The Arrhenius relationship plot of HAp formation.

4. Conclusion

The wet chemical precipitation with the aid of ultrasonic irradiation on aqueous solutions provides a simple and economic route for synthesis of needle-like hydroxyapatite nanoparticles. With the increase of preparation temperature and reaction time, the HAp content increases. The adding of carbamide during the preparation process is important for the formation of HAp nanoparticles. An Arrhenius relationship was found between the HAp formation rate and the reaction temperature. The activation energy of the formation of HAp nano-particles under ultrasonic irradiation was calculated to be 59.9 kJ/mol.

Acknowledgement

This study was supported by the Chinese National Natural Science Foundation of ShaanXi Province.

References

[1] K.J.L. Burg, S. Porter, J.F. Kellam, Biomaterial development for bone tissue engineering, Biomaterials 21 (2000) 2347–2359.
[2] A.K. Dash, G.C. Cudworth, Therapeutic applications of implantable drug delivery systems, J. Pharmacol. Toxicol. Method 40 (1998) 1–12.
[3] W. Suchanek, M. Yoshimura, Processing and properties of hydroxyapatite-based biomaterials for use as hard tissue replacement implants, J. Mater. Res. 13 (1998) 94–117.
[4] D.M. Liu, Preparation and characterization of porous hydroxyapatite bioceramics via a slip-casting route, Ceram. Int. 24 (1998) 441–446.
[5] G. Bezzi, G. Celotti, E. Landi, T.M.G. La Torretta, I. Sopyan, A. Tampieri, A novel sol–gel technique for hydroxyapatite preparation, Mater. Chem. Phys. 78 (2003) 816–824.
[6] H.Q. Zhang, S.P. Li, Y.H. Yan, Dissolution behavior of hydroxyapatite in hydrothermal solution, Ceram. Int. 27 (2001) 451–454.
[7] H.S. Liu, T.S. Chin, L.S. Lai, S.Y. Chiu, K.H. Chuang, C.S. Chang, M.T. Lui, Hydroxyapatite synthesized by a simplified hydrothermal method, Ceram. Int. 23 (1997) 19–25.
[8] M. Toriyama, A. Ravaglioli, A. Krajewski, G. Celotti, A. Piancastelli, Synthesis of hydroxyapatite-based powders by mechno-chemical method and their sintering, J. Eur. Ceram. Soc. 16 (1996) 429–436.
[9] R. Kumar, P. Cheang, K.A. Khor, RF plasma processing of ultra-fine hydroxyapatite powders, J. Mater. Process Technol. 113 (2001) 456–462.
[10] P. Luo, T.G. Nieh, Synthesis of ultrafine hydroxyapatite particles by a spray dry method, Mater. Sci. Eng. C 3 (1995) 75–78.
[11] A. Cuneyt Tas, Combustion synthesis of calcium phosphate bioceramic powders, J. Eur. Ceram. Soc. 20 (2000) 2389–2394.
[12] V. Shukla, G.S. Elliott, B.H. Kear, Hyperkinetic deposition of nanopowders by supersonic rectangular jet impingement, Scripta Mater. 44 (2001) 2179–2182.
[13] K. Itatani, K. Iwafune, F. Scott Howell, M. Aizawa, Preparation of various calcium-phosphate powders by ultrasonic spray freeze-drying technique, Mater. Res. Bull. 35 (2000) 575–585.
[14] S. Raynaud, E. Champion, D. Bernache-Assollant, P. Thomas, Calcium phosphate apatites with variable Ca/P atomic ratio. I. Synthesis, characterization and thermal stability of powders, Biomaterials 23 (2002) 1065–1072.
[15] J.C. Knowles, S. Callcut, G. Georgiou, Characterisation of the rheological properties and zeta potential of a range of hydroxyapatite powders, Biomaterials 21 (2000) 1387–1392.
[16] Y.X. Pang, X. Bao, Influence of temperature, ripening time and calcination on the morphology and crystallinity of hydroxyapatite nanoparticles, J. Eur. Ceram. Soc. 23 (2003) 1697–1704.